The connectedness of Energy Transition Metals

Andrea Bastianin[a,c] Chiara Casoli[c,*] Marzio Galeotti[b,c]

March 27, 2023

Abstract: We assess the degree of spillovers or connectedness among the 16 constituents of the IMF's Energy Transition Metals (ETMs) index. We rely on regularized estimation of Vector Autoregressive (VAR) models and generalised forecast error decomposition to quantify spillovers among ETMs. By calculating both static and dynamic measures of connectedness for commodity returns and volatilities, we can gain insight into the patterns of shock transmission within the ETMs. Our static analysis reveals that base and precious metals are net shock transmitters, while minor and most battery metals are net receivers. Looking at the dynamics of connectedness with a rolling window estimation of the VAR, we find that the system-wide, within-group, and between-group connectedness measures are all time-varying. Notably, the aftermath of the COVID-19 pandemic has seen a rising trend in the connectedness between precious and base metals and other ETMs. To gain economic intuition for these dynamics, we correlate measures of connectedness with proxies of global economic activity, uncertainty, and supply chain pressures. Our findings suggest that fluctuations in connectedness may be linked to broader economic trends. Overall, our study provides valuable insights into the interconnectedness of ETMs and the ways in which shocks can propagate across different markets.

Key Words: Connectedness; Energy Transition; Metals; Raw materials.

JEL Codes: Q02; Q41; Q43.

[a] Department of Economics, Management, and Quantitative Methods, University of Milan, Milan, Italy.

[b] Department of Environmental Science and Policy, University of Milan, Milan, Italy.

[c] Fondazione Eni Enrico Mattei, Milan, Italy.

[*] *Corresponding author*: Chiara Casoli, Fondazione Eni Enrico Mattei, Corso Magenta, 63, 20123, Milan, Italy. Email: `chiara.casoli@feem.it`.

1 Introduction

Critical raw materials (CRMs) are increasingly relevant in several technological domains and having access to them might soon become as essential as having access to reliable energy supplies. Broadly speaking, CRMs are economically and strategically important raw materials characterized by a low degree of substitutability and high-supply risk. Lists of CRMs are compiled and regularly updated by many governmental agencies (see e.g. U.S. Department of the Interior, 2022; European Commission, 2020b; Nakano, 2021). European Commission President von der Leyen announced a "CRMs act" in her 2022 State of the EU address to tackle the growing importance of CRMs for achieving key policy targets, including the twin green and digital transition.[1]

CRMs threat supply chains and hence might hamper the large scale deployment of technologies in strategic sectors such as renewable energy, e-mobility, defence and aerospace (European Commission, 2020a). In this paper we focus on a subset of raw materials – *Energy Transition Metals* (ETMs) – that are input in the production of clean energy technologies such as solar, wind, batteries and fuel cells. Borrowing from the burgeoning literature on energy security, we can conceptualize ETMs security focusing on four dimensions: availability, affordability, efficiency, and environmental stewardship (see e.g. Metcalf, 2014; Sovacool and Brown, 2010). While ETMs exhibit criticalities related to all of such dimensions, we mainly focus on the interplay between availability and affordability.[2]

In terms of availability – defined as the ability to procure a sufficient, safe and diversified supply of ETMs – Table 1 shows that the production of most of the metals considered in this study is highly concentrated geographically, often in poor or developing countries. Affordability relates – among other things – to the provision of ETMs at stable prices (Yergin, 2006). As shown in Figure 1 the prices of ETMs are highly volatile. Availability and affordability factors are intertwined and both help explaining a large part of the volatility observed in the prices of ETMs. In fact, the combination of low substitutability, low price elasticity of supply and demand and a high concentration of production in few countries

[1]See `https://ec.europa.eu/commission/presscorner/detail/ov/speech_22_5493`.

[2]See Lèbre et al. (2020), Owen et al. (2022) and Zhang et al. (2022) for a broader perspective.

implies that even small shocks arising on either side of the markets for ETMs can trigger large price responses (Boer et al., 2021; Fally and Sayre, 2018; Graedel et al., 2015a,b).

The existence of liquid futures markets – performing their functions of price discovery and risk mitigation – for ETMs could in principle contribute to ETM security by improving their affordability for different classes of stakeholders, ranging from firms along the supply chain of key technologies to countries. However, while for some of the ETMs in our sample derivative markets are liquid and have a long history (e.g. many base and precious metals), most of the metals that are in high demand for clean energy technologies, such as cobalt or rare earth elements, do not have well developed futures markets.

We assess the degree of spillovers or connectedness among the 16 constituents of the IMF's ETM index. By calculating both static and dynamic measures of connectedness for commodity returns and volatilities, we can gain insight into the patterns of shock transmission within the ETMs. In this paper we follow the methodology put forth by Diebold and Yilmaz (2009, 2012, 2014) and rely on a Generalised Variance Decomposition (GFEVD) from VAR models to construct measures of directional spillovers among ETMs.

Alternatives ways to measure connectedness have been proposed in the literature. An incomplete list of these alternative methods include principal components analysis and Granger-causality approach of Billio et al. (2012) and the approach based on network analysys techniques for time-series due to Barigozzi and Brownlees (2019); Barigozzi et al. (2022). Moreover, other methods focus on the asymmetry of connectedness at different frequencies or quantiles of the distribution (e.g. Baruník and Křehlík, 2018; Baruník and Kley, 2019; Zhu et al., 2019).

GFEVD-based connectedness is probably the most widely used approach and has the advantage of measuring spillover from each commodity to others without identification assumptions or imposing a particular ordering of the endogenous variables in the VAR (see Koop et al., 1996; Pesaran and Shin, 1998). Moreover, Diebold and Yilmaz (2014) highlight the close relationship between connectedness measures based on GFEVD and key statistics used in the field of network analysis. Estimating network effects is crucial because it is well recognized that sectoral microeconomic shocks can propagate and eventually result in aggregate fluctuations (see Acemoglu et al., 2012, as an example), and contagion from a large number of entities or markets may result in systemic crises (Bandt et al., 2012).

An application of the GFEVD-based methodology to commodity connectdness, focusing on volatility spillovers, is provided by Diebold et al. (2018). Recent surveys of the literature dealing with this methodology are provided by Balcilar et al. (2022) and Diebold and Yilmaz (2023). As far as we know this paper is the first to focus on the connectedness of a large set of ETMs. Measuring ETM connectdness is central for risk measurement and management both from the perspective of private sector investment (e.g. for producers of clean energy technologies) and for the formulation of public policies (e.g. connectedness tends to increase during commodity-market crises).

The rest of the paper is organized as follows. Section 2 describes data and econometrics methods underlying our analysis; Section 3 presents our main results while Section 4 concludes. An Appendix with further details and results completes the paper.

2 Data and methods

2.1 Data

We source daily prices for 16 metals from Refinitiv Eikon. We analyse 7 base metals, 3 precious metals and 6 other minerals, that we define generically as "other ETMs". These metals are the constituents of the International Monetary Fund's ETMs price index . Table 1 shows the list of commodities and the clean energy technologies for which they are used. This table also reports the weight of each commodity in IMF-ETMs price index that is based on the share of imports of each metal in total world commodity imports. As we can see, traditional base metals – such as aluminium and copper – with a wide range of industrial uses, get most of the weight in the IMF index. On the contrary, cobalt, rare earth elements (REE), lithium and other minor metals – chiefly used in clean energy technologies – represent a small share of global imports.[3] Table 1 also reveals that the production of most minor metals is highly geographically concentrated. For instance over 60% of the world production of REE, silicon and vanadium is concentrated in China, while the Democratic Republic of

[3]Some of these metals – such as cobalt, copper, nickel, lithium and manganese – are referred to as battery metals.

Congo is the leader producer of cobalt.

Table 1: Energy transition metals: classification. sources and uses

Metal	Group	IMF weight %	Top Producer (% world)	Main Uses
Aluminum	Base	15.9	Australia (28)	All sectors
Cobalt	Base	0.6	Congo (DRC) (71)	Li-ion batteries. Fuel Cells
Copper	Base	34.3	Chile (26)	All sectors
Lead	Base	3.8	China (47)	Wind. PV
Molybdenum	Base	5.3	China (43)	Wind. PV
Nickel	Base	6.7	Indonesia (37)	Li-ion batteries. Fuel Cells. PV. Wind
Zinc	Base	6.1	China (32)	PV
Palladium	Precious	3.1	South Africa (40)	Fuel Cells
Platinum	Precious	4.4	South Africa (72)	Fuel Cells
Silver	Precious	7.0	Mexico (23)	Fuel Cells. PV
Chromium	Other	3.2	South Africa (44)	Fuel cells. Wind
Lithium	Other	0.3	Australia (55)	Li-ion batteries
Manganese	Other	3.7	South Africa (37)	Wind. Li-ion batteries
REE	Other	0.5	China (60)	Wind. EV
Silicon	Other	5.1	China (71)	Li-ion batteries
Vanadium	Other	0.2	China (66)	Fuel Cells

Notes: data on the leading producing countries and the relative production as a share of world total are provided by the USGS in the Mineral Commodity Summaries 2022 report. The main uses for each mineral are taken from the Critical Raw Materials for Strategic Technologies and Sectors in the EU report by the European Commission and refer to the use within the European Union. IMF weights represent the share of imports of metal m in total global commodity import

Some base and precious metals in our sample have been traded in future exchanges for many years, while other minerals – notably those labelled as "other ETMs" in the second column of Table 1 – have a much shorter price history. The low liquidity of markets for these ETMs implies that their prices change infrequently and hence working with daily or weekly data is unfeasible. Daily data are then aggregated to construct monthly returns and realized volatilities (RV) that span a sample running from June 2012 to December 2022, for a total of 127 observations. Denoting daily real prices for metal m as P_{m,t_d} and daily log-returns as $r_{m,t_d} = 100 \times \log(P_{m,t_d}/P_{m,t_d-1})$, we compute monthly RV as follows:[4]

$$RV_{m,t} = \frac{1}{D_t} \sum_{t_d=1}^{D_t} r^2_{m,t_d}, \tag{1}$$

where D_t is the number of days in month t. In subsequent analyses we rely on monthly

[4]Daily prices are deflated using the interpolated Consumer Price Index for the US.

real returns $r_{m,t} = (1/D_t) \sum_{t_d=1}^{D_t} r_{m,t_d}$ and $\log \sqrt{RV_{m,t}}$. We consider log of realized standard deviations in that RV_t is extremely skewed, while $\log \sqrt{RV_{m,t}}$ is approximately Gaussian for most commodities (see Andersen et al., 2001; French et al., 1987, for a discussion in the context of stock market volatilities). For simplicity, from now on we keep on using the shorthand notation RV, even though we rely on $\log \sqrt{RV_{m,t}}$ in the analyses.

Figure 1: Price of Energy Transition Metals: June 2012 - December 2022

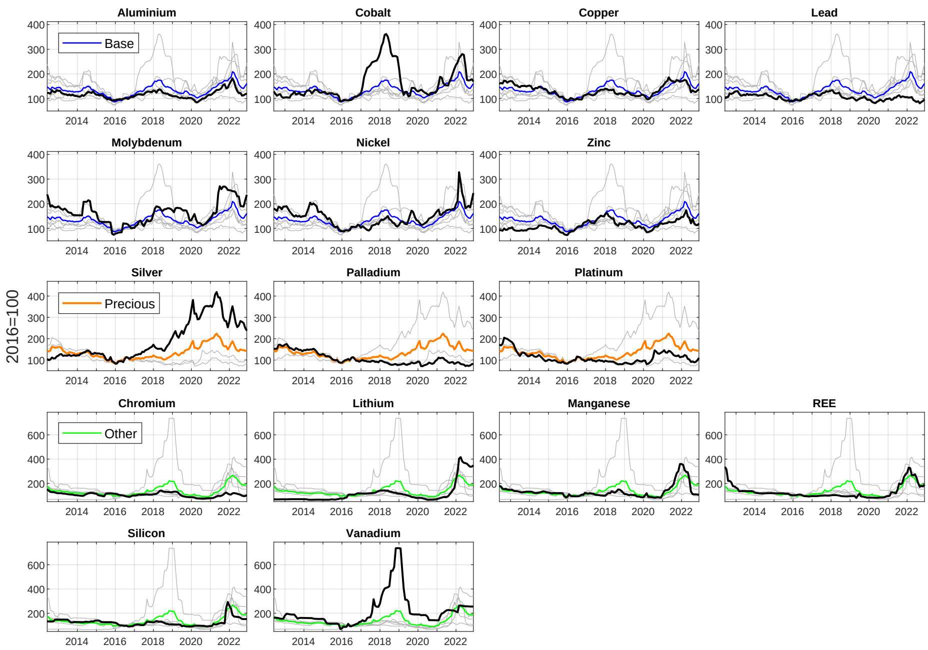

Notes: for each commodity, the figure shows its price (black line) and the price index for the category of metals (coloured line) to which it belongs. Prices have been normalised as follows: $100 \times P_{mt}/\bar{P}_m^{2016}$ where $\bar{P}_m^{2016}$ is the average price of m for 2016. Metal groups are defined in Table 1.

Figure 1 shows the real prices of ETMs in our sample. The prices of base metals, reported in first two rows of the figure, exhibit some cycles and are tend to be higher at the end of the sample. Among precious metals – shown on the third row of Figure 1 – silver displays the largest surge during the second part of the sample. Finally, other ETMs prices are in general characterised by less variability, and for the majority of them there is evidence for a price increase after the COVID-19 pandemic. The only exception is vanadium price, exhibiting a remarkable spike between 2017 and 2020. Such a spectacular rise is due to a set of events affecting both the supply and demand-side of the Chinese market. First, in 2017 China enforced stricter environmental rules; as a consequence, inspections led to temporarily or even permanently, close some vanadium producers. Moreover, in 2018, China released a new standard for high-strength reinforcing bars. These were required to have a higher percentage of vanadium and hence increased overall domestic consumption of this metal. Further graphs and details about the data are reported in Appendix A.

2.2 VAR estimation

Our measures of connectedness are obtained with the following procedure:

1. Estimation of Vector Autoregressive models of order p – VAR(p) – for returns and RV.

2. Computation the connectedness measures based on the generalised forecast error variance decomposition (GFEVD). See Section 2.3

To obtain connectedness measures based on the GFEVD, the first step is to estimate VAR models for monthly returns and RV of 16 ETM. While we do include a constant in our specification, for ease of notation we now consider a zero-mean VAR process:

$$\mathbf{y}_t = \sum_{\ell=1}^{p} \mathbf{A}_\ell \mathbf{y}_{t-\ell} + \mathbf{u}_t, \tag{2}$$

where $\mathbf{y}_t$ is an $M \times 1$ vector with the m-th element corresponding either to r_t^m or $\log \sqrt{RV_{m,t}}$, $\mathbf{u}_t \sim (\mathbf{0}, \mathbf{\Sigma})$ and $\mathbf{A}_\ell$ is an $M \times M$ matrix of coefficients. The choice of the lag order, p, is critical in that the number of coefficients to be estimated is $M + M^2 p$ and hence grows quadratically with p. For instance, with $M = 16$, a VAR(3) model involves estimating 784 coefficients.

We handle dimensionality issues estimating VAR models with an adaptive elastic-net penalty (Zou and Zhang, 2009) which involves both shrinkage and selection. The penalised estimation approach induces sparsity in the coefficient matrices $\mathbf{A}_\ell$. As noted in Nicholson et al. (2017), taking into account the sparsity patterns allows to address over-parametrisation in VAR models without having to select a low lag order p. In low-dimensional settings, the VAR model in Equation (2) is estimated via Ordinary Least Squares. However, as M and p increase, reducing the parameter space of the VAR becomes essential. The adaptive elastic-net consists in adding to Equation (2) an appropriate penalty term. Specifically, fitting a sparse VAR involves solving the following penalised estimation problem:

$$\min_{\mathbf{A}} \sum_{t=1}^{T} \left|\left| \mathbf{y}_t - \sum_{\ell=1}^{p} \mathbf{A}_\ell \mathbf{y}_{t-\ell} \right|\right|_F^2 + \lambda \mathcal{P}_y(\mathbf{A}) \quad \text{for } \lambda \geq 0, \tag{3}$$

where $||\cdot||_F$ denotes the Frobenius norm[5] and $\mathcal{P}_y(\mathbf{A})$ represents the penalty structure applied to the coefficient matrices $\mathbf{A} = [\mathbf{A}_1, \ldots, \mathbf{A}_p]$. The adaptive elastic-net VAR estimator is imposes the following penalty to Equation (3):

$$\mathcal{P}_y(\mathbf{A}) = \alpha||\mathbf{A}||_1 + (1-\alpha)||\mathbf{A}||_2^2, \quad \text{for } 0 \leq \alpha \leq 1. \tag{4}$$

The parameter α measures the trade-off between LASSO and ridge penalties in Equation (4). When $\alpha = 1$, the penalty function yields the LASSO estimator (Tibshirani, 1996). On the other hand, as $\alpha \to 0$, the LASSO penalty shrinks toward 0, the elastic-net becomes closer to ridge regression (Hoerl and Kennard, 1988). The optimal penalty parameters λ and α can be determined using cross-validation, allowing for a completely data-driven approach.[6]

Figure 2 shows the sparsity pattern for the estimated matrices of coefficients in the case of a VAR(4) for returns. As we can see, elements along the main diagonal of $\hat{A}_1$ have darker shades, while off-diagonal elements are often shrunk toward zero. It is worth noting that within this framework, VAR(p) denotes a VAR with a lag order at most equal to p, and the effective lag order is determined equation by equation by the penalty function (see Nicholson et al., 2017, for further details).

---

[5] We make use to the following definitions. The Frobenius norm of an $(Z \times K)$ matrix $\mathbf{B}$ is defined as $||\mathbf{B}||_F = \sqrt{\sum_{z=1}^{Z}\sum_{k=1}^{K}|b_{zk}|^2}$. The 1-norm is $||\mathbf{B}||_1 = \max_{1\leq k \leq K} \sum_{z=1}^{Z}|b_{zk}|$ and the 2-norm can be written as $||\mathbf{B}||_2 = \sqrt{\lambda_{max}\mathbf{B}^*\mathbf{B}}$, where λ_{max} is the maximum eigenvalue of $\mathbf{B}^*\mathbf{B}$ and $\mathbf{B}^*$ is the conjugate transpose of $\mathbf{B}$.

[6] We set α equal to $(1+M)^{-1} \approx 0.059$. Then, the optimal $\hat{\lambda}$ is selected from a grid of values $\lambda_1, \ldots \lambda_n$ via a rolling procedure, between times $T_1 = T/3$ and $T_2 = 2T/3$. The final $\hat{\lambda}$ is the value that minimises the Mean Squared Forecast Error. The grid of values for the choice of $\hat{\lambda}$ is specified by selecting the grid depth and the number of grid values. We set for the returns analysis the grid depth at 50 and the number of values to 10, whereas for RV we opt for an increased grid depth of 500.

Figure 2: VAR model for returns: sparsity

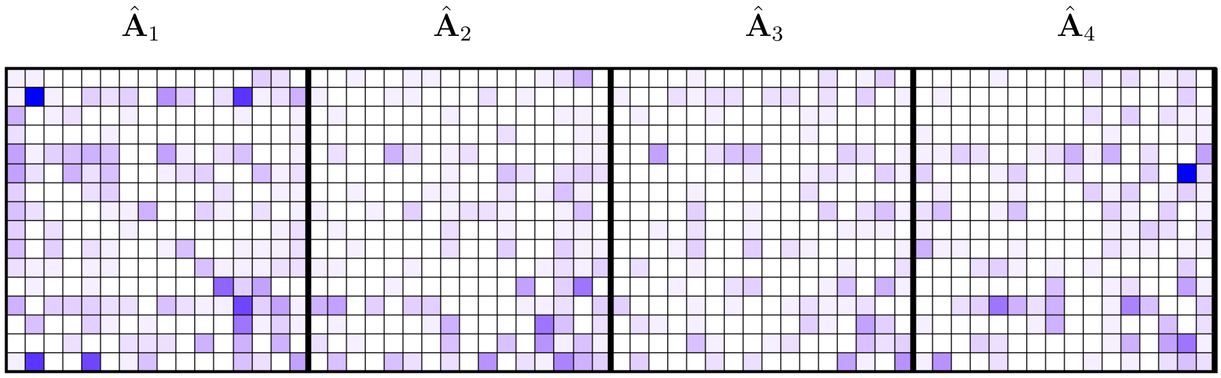

Notes: colored shades indicate active coefficients, with darker shades referring to parameters that are larger in magnitude. White areas denotes coefficients that have been set to zero.

2.3 Measuring connectedness

Our connectedness analysis relies the GFEVD of the VAR as proposed by Diebold and Yilmaz (2009, 2012, 2014) in a series of papers. The GFEVD does not require orthogonalising shocks and is invariant to the ordering of the variables in the VAR:

$$\theta_{ij}(H) = \frac{\sigma_{jj}^{-1} \sum_{h=0}^{H-1} \left(\mathbf{e}_i' \mathbf{\Phi}_h \mathbf{\Sigma} \mathbf{e}_j\right)^2}{\sum_{h=0}^{H-1} \left(\mathbf{e}_i' \mathbf{\Phi}_h \mathbf{\Sigma} \mathbf{\Phi}_h' \mathbf{e}_i\right)} \quad H = 1, 2, \ldots \text{ and } i, j = 1, ..., N \tag{5}$$

where $\mathbf{\Sigma}$ is the covariance matrix of the σ_{jj} the standard deviation of the disturbance of the j-th equation, $\mathbf{e}_j$ is a selection vector with one as j-th element and zero otherwise and the matrices $\mathbf{\Phi}_k$ are derived from the moving average representation of the VAR model in Equation (2).[7] Since the variance shares do not sum to one (i.e. $\sum_{j=1}^{M} \theta_{ij}(H) \neq 1$), we consider the following normalization:

$$C_{i \leftarrow j}^{H} \equiv \tilde{\theta}_{ij}(H) = 100 \times \frac{\theta_{ij}(H)}{\sum_{j=1}^{N} \theta_{ij}(H)}. \tag{6}$$

The generic element $C_{i \leftarrow j}^{H} \equiv \tilde{\theta}_{ij}(H)$ is a measure of (gross) pairwise directional connectedness from j to i; it measures the percentage contribution of mineral j to mineral's i generalised forecast error at horizon H. Note that in general $C_{i \leftarrow j}^{H} \neq C_{j \leftarrow i}^{H}$. Armed with pairwise directional connectdness measures, we can compute the following statistics (from now on we

[7] A stable VAR process can be rewritten in moving average form as follows: $\mathbf{y}_t = \sum_{k=0}^{\infty} \mathbf{\Phi}_k \mathbf{u}_{t-k}$, where $\mathbf{\Phi}_0 = I_M$ and $\mathbf{\Phi}_k = \sum_{\ell=1}^{k} \mathbf{\Phi}_{k-\ell} \mathbf{A}_\ell$ for $k = 1, 2, \ldots$ and $\mathbf{A}_\ell = \mathbf{0}$ for $k > p$.

drop the H superscript for ease of notation):

$$C_{ij} = C_{j \leftarrow i} - C_{i \leftarrow j} \qquad \text{(Net-Pairwise)} \tag{7}$$

$$C_{i \leftarrow \bullet} = \frac{1}{M} \sum_{\substack{j=1 \\ i \neq j}}^{M} \tilde{\theta}_{ij}(H) \qquad \text{(From)} \tag{8}$$

$$C_{\bullet \leftarrow j} = \frac{1}{M} \sum_{\substack{i=1 \\ i \neq j}}^{M} \tilde{\theta}_{ij}(H) \qquad \text{(To)} \tag{9}$$

$$C_i = C_{\bullet \leftarrow i} - C_{i \leftarrow \bullet} \quad \text{(Net)} \tag{10}$$

$$C = \frac{1}{M} \sum_{i=1}^{M} \sum_{\substack{j=1 \\ i \neq j}}^{M} \tilde{\theta}_{ij}(H) \qquad \text{(Total).} \tag{11}$$

Notice that *net pairwise connectedness* in Equation (7) differs from gross pairwise directional connectedness in Equation (6). First, while there are $(M^2 - M)/2$ net pairwise connectedness measures, there are M^2 gross pairwise connectedness measures. In our framework, "gross" pairwise directional connectedness represents a measure of bilateral spillovers, whereas its "net" counterpart allows to divide minerals into net receivers and net transmitters of shocks.

Measures in Equation (8) and (9) are often labelled respectively as "*from*" and "*to*" connectedness, since they define the transmitted and the received spillover for the i-th mineral, and correspond to the off-diagonal row and column sums of the connectedness table. *Total* or *system-wide* connectedness simply corresponds to the sum of *from* – or *to*, equivalently – directional connectedness. Note that $\sum_{j=1}^{M} C_{\bullet \leftarrow j} = \sum_{i=1}^{M} C_{i \leftarrow \bullet} = C$.

Connectedness and network analysis. The connectedness table, (CT), is a $(M+1) \times (M+1)$ matrix with $C_{i \leftarrow j}$ in the first M rows and columns. The $M+1$-th column (row) reports from (to) connectedness, while system-wide connedctedness appears in the lower right corner. Diebold and Yilmaz (2014) show that the GFEVD represents the adjacency matrix of a directed weighted network.[8] Specifically, the GFEVD delivers a matrix whose entries capture the strength and direction of spillovers between commodities. Moreover, it can be shown

[8]Note that, in general, a graph or adjacency matrix $\mathcal{A}$ has elements a_{ij} that indicate edges from i to j. On the contrary, in our approach each entries of the CT measures a spillover from j to i.

that from, to and system-wide connectedness are equivalent to key statistics used in the network literature (e.g. in-degrees, out-degrees and mean degree).

Connectedness within and across groups. In order to capture the differential impact of different groups of commodities, the connectedness table (CT) is aggregated into blocks that correspond to base, precious, and other metals, respectively. To this end, we define a group index vector $\mathbf{G}$ of size $(M \times 1)$ that assigns each of the M commodities to a group $g = 1, 2, 3$.[9] To compute the *within-group connectedness* of each group, we sum all the elements in the connectedness table that pertain to that group, net of the contribution of own shocks to GFEVD:

$$C_{g \leftarrow g} = \frac{1}{M} \sum_{i=1}^{M} \sum_{\substack{j=1 \\ j \neq i}}^{M} C_{i \leftarrow j} \cdot I(G_i = g) \cdot I(G_j = g), \quad \text{for } g = 1, 2, 3, \tag{12}$$

where $I(G_i = g)$ is an indicator function that is equal to 1 if $G_i = g$ and 0 otherwise. Summing over g we get the *system-wise within-group connectedness*: $C_{within} = \sum_{g=1}^{3} C_{g \leftarrow g}$. *Connectedness across groups* can be defined as follows:

$$C_{k \leftarrow z} = \frac{1}{M} \sum_{i=1}^{M} \sum_{j=1}^{M} C_{i \leftarrow j} \cdot I(G_i = k) \cdot I(G_j = z), \quad \text{for } k, z = 1, 2, 3 \text{ with } k \neq z. \tag{13}$$

Notice that with three groups there are 6 different cross-group connectedness measures. System-wide cross-group connectedness is equal to $C_{between} = \sum_{k=1}^{3} \sum_{\substack{z=1 \\ k \neq z}}^{3} C_{k \leftarrow z}$. It follows that: $C = C_{within} + C_{between}$. The distinction between connectedness within and across groups is illustrated in Figure 3.

To and from group-connectedness. To connectedness for group g is simply the sum of to connectedness for metals in group g:

$$C_{\bullet \leftarrow g} = \sum_{j=1}^{M} C_{\bullet \leftarrow j} \cdot I(G_j = g). \tag{14}$$

[9] In our setting, the commodities are ordered according to the group they belong to, with the first 7 entries of $\mathbf{G}$ identifying base metals and being equal to one, entries 8-10 identifying precious metals and being equal to two, and the remaining 6 entries identifying other metals and being equal to three.

Similarly, from connectedness for groups is:

$$C_{g \leftarrow \bullet} = \sum_{i=1}^{M} C_{i \leftarrow \bullet} \cdot I(G_i = g) \tag{15}$$

It follows that $C = \sum_{g=1}^{3} C_{\bullet \leftarrow g} = \sum_{g=1}^{3} C_{g \leftarrow \bullet}$.

Figure 3: Connectedntess within and between groups

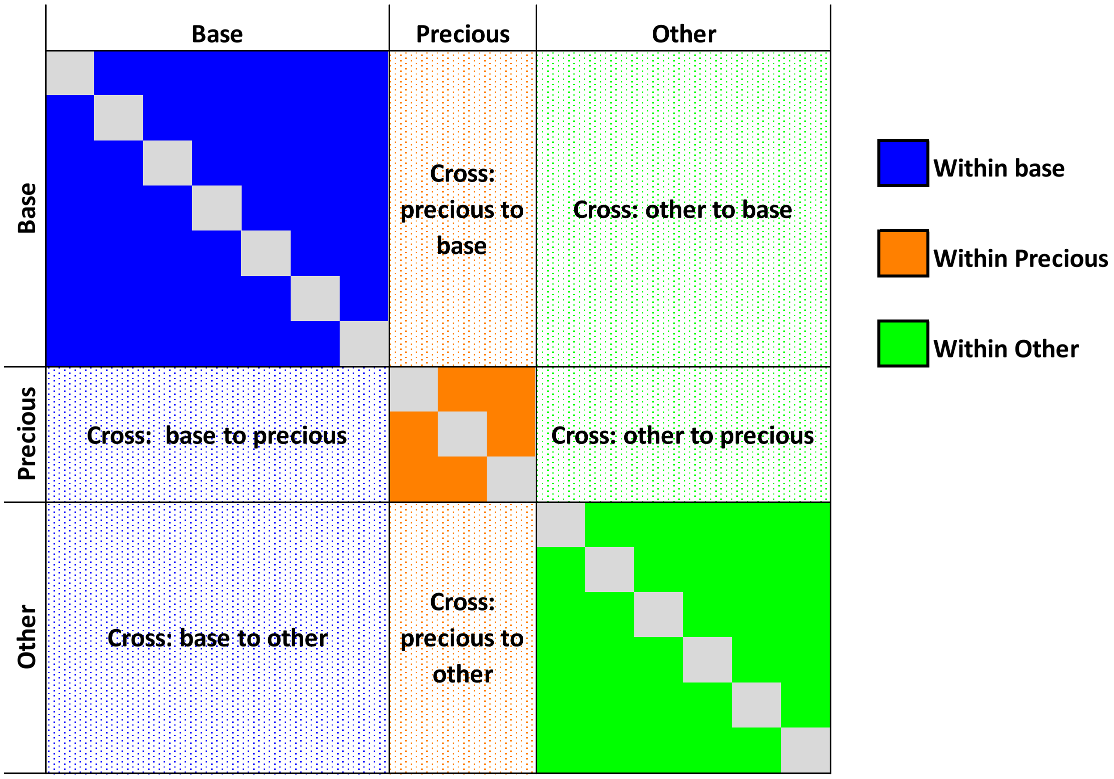

3 Results

The VAR lag order, p, is equal to 4 in the case of returns, whereas we set $p = 3$ for RV. We report results based on the GFEVD at $H = 3$ months horizon.[10] Since returns and volatilities measure different economic concepts, so does connectedness among them. Connectedness

[10]We have increased p up to 12, but this leads to a very low fraction of active coefficients, resulting in a highly sparse VAR. We conclude that 4 lags capture an adequate amount of autocorrelation in the case of ETM returns, while for RV, exhibiting larger sparsity, 3 lags are sufficient. As a robustness check, we have also computed system-wide connectedness considering different horizons. Specifically, we set $H = 4, 6, 12$, and conclude that connectedness of both returns and RV is not particularly sensitive to the choice of H. These results are available from the authors upon request.

for returns relates to changes in expectations, whereas connectedness for volatilities captures the fear and uncertainty of investors.

While we highlight the differences between results when appropriate, we mainly focus on connectedness for volatilities. We give more weight to the analysis of volatility connectedness for two reasons. Firstly, when examining groups as well as individual ETMs, the static analysis of connectedness for volatilities and returns produce comparable results. Secondly, understanding volatility connectedness is critical for real-time crisis monitoring. In fact, volatilities tend to move together only during times of crises and are often more responsive than returns which, on the contrary, move together in both downturns and upswings. The full set of results is available in Appendix B.

3.1 Full sample connecteness

Starting from the CT, we compute the from, to and net connectedness for RV as defined in Equations (8), (9) and (10) and display them in Figure 4 where base, precious and other ETMs are clustered and represented with different colors.

Figure 4: To, from and net connectedntess – volatilities

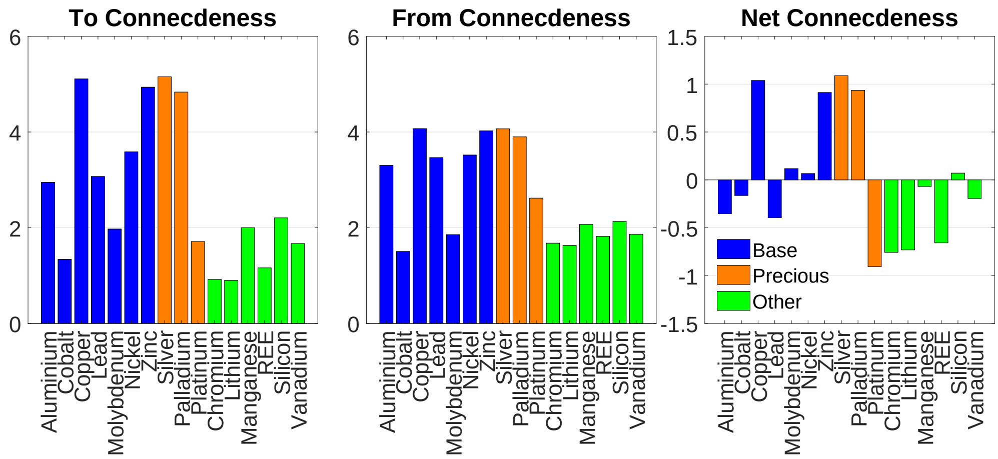

Base and precious metals exhibit greater from and to connectedness, whereas the other ETMs transmit and receive less volatility spillovers. Connectedness is thus stronger for the first two groups, while other ETMs are to some extent less sensitive to base and precious metal market dynamics. Moreover, other ETMs also exhibit a degree of from connectedness that is generally higher than the degree of to connectedness, suggesting that they are net receivers of shocks.

As a matter of fact, metals in the "other ETMs" group – with the exception of silicon – have a negative net directional connectedness, and hence they are net receivers of volatility spillovers. On the contrary, two precious metals out of three - namely, silver and palladium - are net transmitters of shocks. Results for base minerals are mixed, with four out of seven metals being classified as net transmitters of shocks. It is worth noting that copper and zinc have the highest degree of from and to connectedness among base metals. When analysing spillovers for returns, copper is confirmed to be the most connected metal, thus it seems to be the principal driver of markets dynamics for ETMs.

We summarise the full-sample connectedness analysis for volatilities in Figure 5. The heatmap in Figure 5a represents the volatility CT for groups of ETMs. Within-group connectedness (net of own connectedness for each metal) can be read along the main diagonal, while off-diagonal elements of the heatmap capture volatility spillovers across groups. Within-group spillovers are largest for base metals, while those for precious and other ETMs are much smaller and comparable in magnitude; this suggests that these two markets receive a large share of volatility spillovers from the base metal group. Figure 5b reports the to, from and net group-connectedness, confirming the results obtained with individual commodities. Base and precious metals are overall net transmitters, while other ETMs are net receivers of shocks.

Some interesting facts also emerge from the CT for volatilities that appears in Appendix A. Diagonal elements are in general lower for base and precious metals, and higher for minerals classified as "other ETMs". This means that other ETMs variability is more self-explained with respect to the other two metal categories. The only exception is molybdenum that, notwithstanding being classified as base metal, has a degree of self-explained volatility as high as other ETMs. Off-diagonal elements range from the very high levels of pairwise directional connectedness measured from zinc to lead and from palladium to platinum (more than 20%) to the marginal and often negligible connectedness arising from other ETM to base and precious metals (e.g. silicon and vanadium transmit around 1% of the RV to zinc and silver). Crucially, the opposite is not true, as the connectedness from any of the base and precious metals to other ETM is on average larger, denoting a remarkable asymmetry.

Figure 5: Full sample group connectedness measures for volatility

(a) Within and cross group connectedness (b) To, from and net connectedness

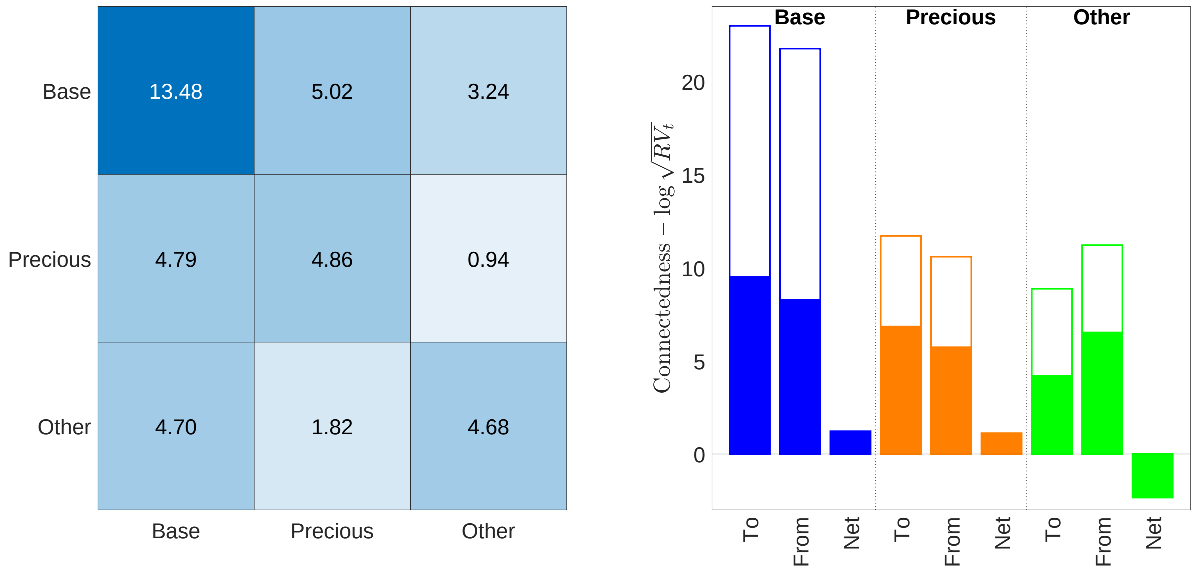

Notes: panel (a) shows within group connectedness along the main diagonal, while off-diagonal elements are cross group connectedness measures. Panel (b) shows the to, from and net connectedness statistics for groups of metals. Colored areas refer to the off-diagonal statistics, whereas the white areas denote the statistics comprehending the diagonal elements.

Since the visualization of the pairwise connectedness measures is easier when represented via network graphs, the remainder of this discussion is delayed to Section 3.2.

Lastly, we focus on full-sample total or system-wide connectedness, as defined in Equation (11), which is equal to 44.93% for returns, and to 43.53% for RV. These results are in line with those of Diebold et al. (2018), estimating a total connectedness among commodity prices at 40%. This implies that almost half of metals variability uncertainty originates by "non-own" shocks. We can further disentangle total volatility connectedness measuring within and between connectedness: 23.02% of the connectedness arises within the same group of ETMs, whereas the 20.51% of system-wide connectedness originates across groups.

3.2 Network visualisation

To better display the results, we consider the network representation of the CT in Figure 6.[11]

[11]We use the Gephi open-access software available at `https://gephi.org/`

Figure 6: Network visualisation for ETMs returns and RV connectedness – June 2012 - December 2022

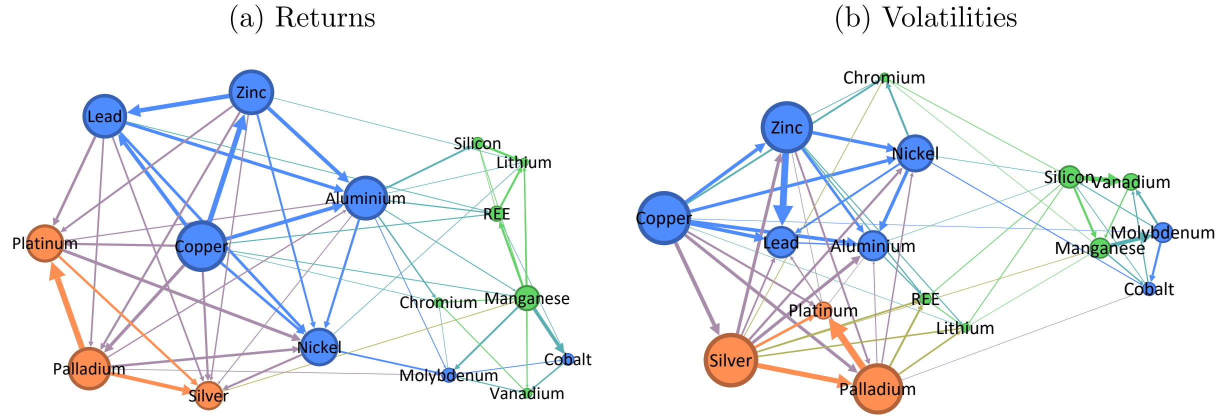

Notes: size of the nodes is determined by to connectedness. Arrows and edges refer to the net-pairwise connectedness above the median.

To improve the network visualisation, we rely on net-pairwise statistics C_{ij} to determine the arrow direction that points towards net receivers of shocks. Visual cluttering is reduced by dropping arrows associated to metals with positive net-pairwise connectedness below the median. The size of arrows and edges is also proportional to net-pairwise connectedness, while node size is determined by to connectedness $C_{\bullet \leftarrow j}$. Lastly, node colour reflects the grouping of metals into base (blue), precious (orange), and others (green). We rely on the ForceAtlas2 algorithm (Jacomy et al., 2014) that finds an equilibrium in which repelling and attractive forces among nodes are balanced. The nodes naturally repulse each other, whereas links attract nodes with different forces, proportional to net-pairwise connectedness.

It is interesting to note that, even though we provide three *ex-ante* defined clusters, the completely data-driven algorithm groups together the base, precious and other ETM metals, both in the case of returns and RV analyses. The only exceptions are given by molybdenum and cobalt, considered as base metals by the IMF but part of the other ETMs according to the connectedness features both in the case of RV and returns connectedness.

As for connectedness for volatilities shown in Figure 6b, chromium, rare earth elements and lithium are closer to base and precious metals, whereas when analysing connectedness in returns, they are grouped among the other ETMs. Base and precious metals have more weight in the network and are more connected than other ETMs. This can be appreciated by focusing on the size of the nodes and the number of arrows originating from each node, respectively.

3.3 Dynamic rolling sample connectedness

Despite the static connectedness analysis provides useful tools to measure the average degree of connectedness, it is important to take into consideration the fact that the degree of connectedness may change over time. Figure 7 reports the system-wide returns and volatility connectedness obtained with a rolling window estimation approach.[12] The figure also highlights important dates associated with key events when we see sudden peaks in connectedness.

Return connectedness from mid-2017 is always above the static full-sample average of 44.93%, suggesting that connectedness among the ETMs was lower in the beginning of the sample (i.e. 2012 – mid-2017) and has recently increased. Before the Covid-19 outbreak, return connectedness seems on a slightly decreasing path, while after the minimum, registered around 2020, there is again a surge in total connectedness among ETMs. Volatility connectedness dynamics is downward sloped until the end of 2020. Thereafter, system-wide connectedness of ETMs RV seem on an increasing trend. Surprisingly, we do not find evidence for an increase in RV connectedness during the only recession within our sample. This may be due to the particular features of the 2020/21 slowdown, characterised by high levels of uncertainty but also by an umprecedent economic freezing (i.e. production, trade and consumption dramatically dropped, affecting almost all markets around the world). The announcement of tarrifs on US aluminium imports by president Trump in March 2018 and the short squeeze in the London Metal Exchange's nickel market in March 2022 are both associated with a subsequent drop of RV connectedness. Other than these metal-related events, RV total connectedness responds negatively to the Brexit confirmation at the end of 2019 and to the Covid-19 spread in March 2020, whereas after the Russian invasion of Ukraine in February 2022 there is a positive peak in connectedness.

[12] We set, as for the static full-sample analysis, a VAR(4) in the case of returns and a VAR(3) for RV, using a rolling window of 60 observations. Finally, we consider $H = 3, 4, 6, 12$, but report only results for $H = 3$ given the marginal and negligible differences in the estimated connectedness.

Figure 7: Retuns and volatility connectedness - rolling sample

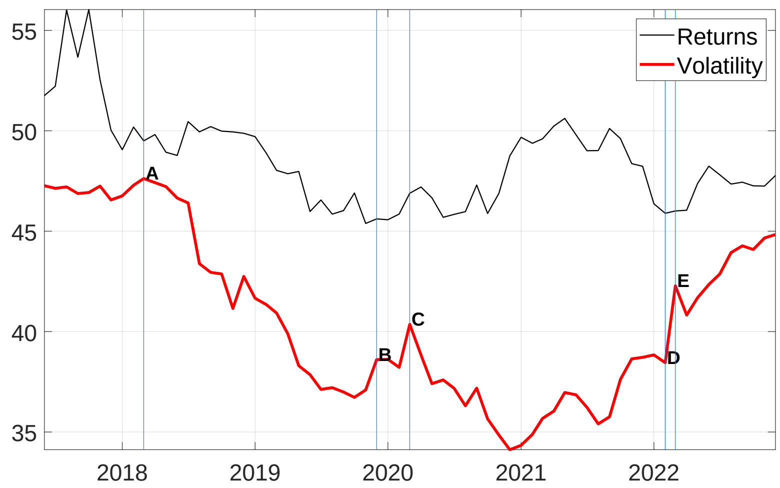

- A: 2018:03 - Tarrifs on Aluminium
- B: 2019:12 - Brexit
- C: 2020:03 - Covid
- D: 2022:02 - War in Ukraine
- E: 2022:03 - Nickel short squeeze

Additionally, we consider the rolling-sample group connectedness for both returns and volatility of ETMs. Main results are shown in Figures A5, reporting the total, within and between system-wide connectedness. It is interesting to note that the total connectedness – both of returns and RV – mimic the evolution of the between connectedness, meaning that cross-group spillovers, rather than within-group ones, are determinant in shaping the final time-varying system-wide connectedness.

Finally, we report in Figure A6 the net connectedness for each cluster of metals. Overall, the dynamics of the total connectedness in returns or RV are closer to the net connectedness of base metals, which shows the same pattern. On the contrary, the evolution of precious metals and other ETMs net connectedness is not in line with the total connectedness fluctuations, either if considering returns or volatilities. We believe this is a further confirmation of the relative importance of base metals in the ETMs system of commodities.

3.4 Drivers of connectedness

To better understand the drivers of total connectedness for ETMs, we consider its correlation with different variables. Specifically, since connectedness in returns should be associated to fluctuations in the business cycle, we focus on the correlation between the estimated time-varying return connectedness (C_t^{ret}) and the Global Economic Conditions Indicator (GECON) of Baumeister et al. (2022). We further examine the correlation between C_t^{ret}

and the Global Supply Chain Pressure Index (GSCPI) of Benigno et al. (2022), since this last indicator should capture fluctuations strongly associated with commodities, including ETMs. As for RV connectedness (C_t^{RV}), we focus on proxies of economic uncertainty. In particular, we analyse the correlation of C_t^{RV} with the Global Economic Policy Uncertainty (GEPU) index (Davis, 2016) and the Trade Policy Uncertainty (TPU) indicator proposed by Caldara et al. (2020).[13] Figure 8 shows the selected indices together with returns and RV time varying connectedness measures.

Figure 8: Time-varying connectedness, economic activity, uncertainty and supply chain pressure

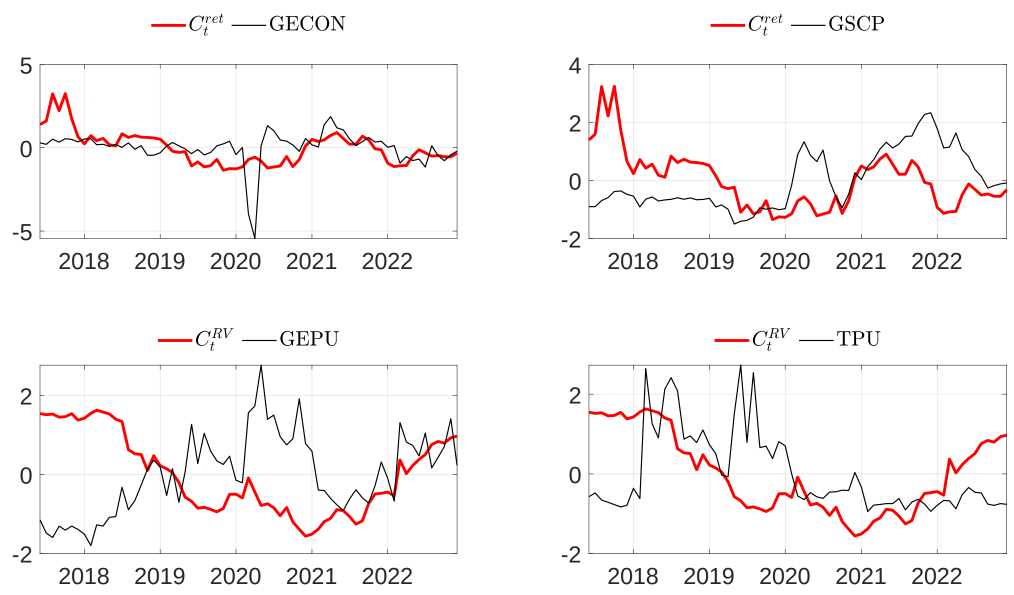

Interestingly, connectedness for returns increases during the Covid-induced recession of 2020, when the GECON index exhibits a severe drop. After the Covid-19 pandemic, however, the degree of connectedness for returns seems positively correlated with the economic activity (top-left panel). On the contrary, we fail to detect statistically significant correlation between connectedness for ETMs returns and the global supply-chain pressure (top-right panel). Focusing on the RV connectedness, it is clearly shown that, whereas at the beginning of the sample C_t^{RV} negatively correlates with the economic uncertainty, starting from the mid-2021

[13]We also consider the VIX index, but since its dynamics are similar to the evolution of the GEPU, we show results considering the GEPU only.

the two indicators are both on a rising pattern (botto-left panel). A similar behaviour is observed also for the VIX index, here not reported to keep the discussion concise. On the contrary, it is hard to detect some kind of co-movement between the trade policy uncertainty indicator and ETMs volatility connectedness (bottom-right panel). By considering a simple leads-and-lags analysis of the correlation coefficients between the time-varying connectedness and the selected measures in Figure 8, we end up to the conclusion that in fact, the only significant drivers of the system-wide connectedness are the GECON, for what concerns C_t^{ret}, and the GEPU, for C_t^{RV} (see Figure A7).

3.5 Alternative measures of connectedness

As a robustness check, we also compare our methodology with an alternative measure of connectedness, specifically we derive the time-varying system-wide connectedness for returns and volatilities by using the Principal Component Analysis, as proposed by Billio et al. (2012). Since the intuition of PCA is that the variance-covariance matrix of the variables can be summarised by the first few eigenvalues, we extract the first principal component as a driver of all the returns and volatilities variation during the rolling sample. This implies that the extracted PCs explain the majority of the common movement between the 16 returns or RV, resulting in a different statistical proxy of the connectedness degree.

Results are reported in Figure 9, showing that connectedness in returns may be affected by different definitions and slightly varies with the two statistical methodologies, whereas the estimates of RV connectedness appear remarkably similar, regardless the used approach. The different dynamics of the two connectedness measures reflect the intrinsic way in which they are built. For instance, while the total connectedness as proposed by Diebold and Yilmaz (2009) sums the received (or transmitted) spillovers for all the considered commodities, the PC-based connectedness extracts the information from a few eigenvalues of the variance-covariance matrix. The evolution of C_t^{ret} reflects most of the movements in base metals net connectedness, as argued above. This comes straightforwardly from the major weight these commodities' spillovers play among all the other considered minerals. On the contrary, the PC-based connectedness of returns seems more in line with the pattern of precious metals

Figure 9: Time-varying connectedness and measures of systemic risk

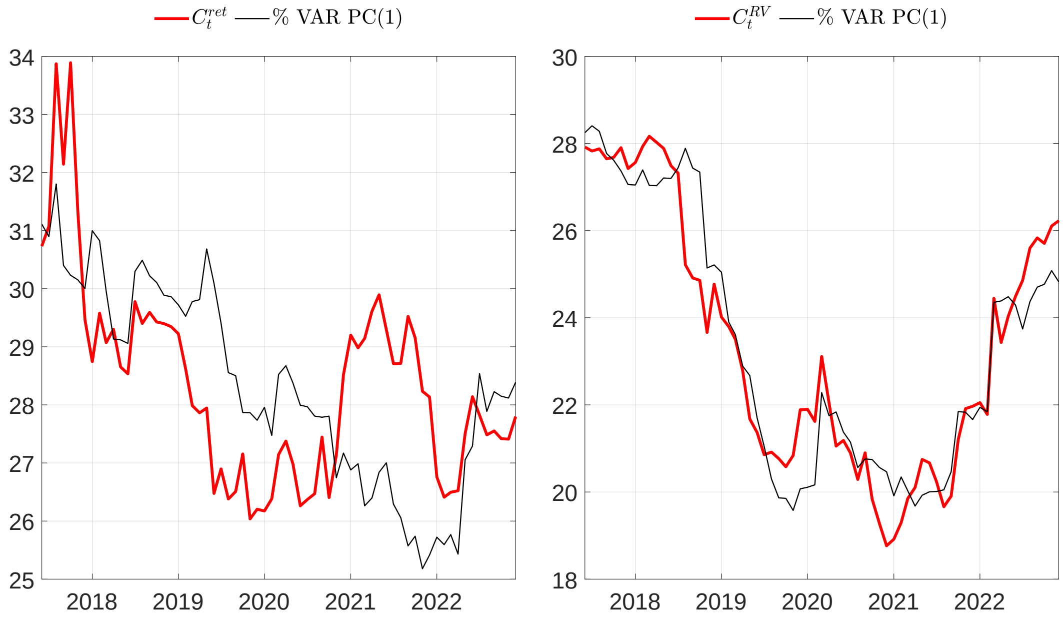

Notes: Since the PCA requires a prior standardisation of the variables, also our measures of connectedness, C_t^{ret} and C_t^{RV} have been rescaled, in order to make the comparison possible.

net connectedness, shown in Figure A6.

4 Conclusions

We have estimated return and volatility spillovers for 16 ETMs relying on the connectedness approach of Diebold and Yilmaz (2009, 2012, 2014). Specifically, we consider a sparse VAR with an elastic-net structure, and then construct our connectedness measures from the Generalised Forecast Error Variance Decomposition, which is independent from variables ordering.

Static full-sample connectedness analysis shows that base and precious metals transmit shocks to the other ETMs that are net receivers. By splitting the 16 commodities in three groups – defined, following the IMF, as base and precious metals, and other ETMs – we demostrate that almost half of the connectedness originates within the group, whereas the other half is due to cross-group spillovers.

Considering the dynamics of connectedness – obtained with a rolling window estimation of the VAR – we demonstrate that the system-wide volatility connectedness has increased after the COVID-19 outbreak. The system-wide connectedness of ETM returns is positively correlated with the economic activity, whereas volatility connectedness seems to be more related to global economic policy uncertainty. Finally, alternative measures of connectedness may lead to slightly different results, but our results seem overall robust to the different definition of connectedness based on principal components.

References

Acemoglu, D., Carvalho, V. M., Ozdaglar, A., and Tahbaz-Salehi, A. (2012). The network origins of aggregate fluctuations. *Econometrica*, 80(5):1977–2016.

Andersen, T. G., Bollerslev, T., Diebold, F. X., and Ebens, H. (2001). The distribution of realized stock return volatility. *Journal of financial economics*, 61(1):43–76.

Balcilar, M., Usman, O., and Agan, B. (2022). On the connectedness of commodity markets: A critical and selective survey of empirical studies and bibliometric analysis. *Journal of Economic Surveys*, *forthcoming*.

Bandt, O. D., Hartmann, P., and Peydró, J. L. (2012). Systemic Risk in Banking: An Update. In Berger, A. N., Molyneux, P., and Wilson, J. O. S., editors, *The Oxford Handbook of Banking*, chapter 25, page 633–672. Oxford University Press.

Barigozzi, M. and Brownlees, C. (2019). Nets: Network estimation for time series. *Journal of Applied Econometrics*, 34(3):347–364.

Barigozzi, M., Cavaliere, G., and Moramarco, G. (2022). Factor network autoregressions. *arXiv preprint arXiv:2208.02925*.

Baruník, J. and Kley, T. (2019). Quantile coherency: A general measure for dependence between cyclical economic variables. *The Econometrics Journal*, 22(2):131–152.

Baruník, J. and Křehlík, T. (2018). Measuring the frequency dynamics of financial connectedness and systemic risk. *Journal of Financial Econometrics*, 16(2):271–296.

Baumeister, C., Korobilis, D., and Lee, T. K. (2022). Energy markets and global economic conditions. *Review of Economics and Statistics*, 104(4):828–844.

Benigno, G., Di Giovanni, J., Groen, J. J., and Noble, A. I. (2022). The GSCPI: a new barometer of global supply chain pressures. Staff Report 1017, Federal Reserve Bank of New York.

Billio, M., Getmansky, M., Lo, A. W., and Pelizzon, L. (2012). Econometric measures of connectedness and systemic risk in the finance and insurance sectors. *Journal of financial economics*, 104(3):535–559.

Boer, L., Pescatori, A., and Stuermer, M. (2021). Energy transition metals. Working Paper 243, International Monetary Fund.

Caldara, D., Iacoviello, M., Molligo, P., Prestipino, A., and Raffo, A. (2020). The economic effects of trade policy uncertainty. *Journal of Monetary Economics*, 109:38–59.

Davis, S. J. (2016). An index of global economic policy uncertainty. Technical report, National Bureau of Economic Research.

Diebold, F. X., Liu, L., and Yilmaz, K. (2018). Commodity Connectedness. In Mendoza, E. G., Pastén, E., and Saravia, D., editors, *Monetary Policy and Global Spillovers: Mechanisms, Effects and Policy Measures*, volume 25 of *Central Banking, Analysis, and Economic Policies Book Series*, chapter 4, pages 97–136. Central Bank of Chile.

Diebold, F. X. and Yilmaz, K. (2009). Measuring financial asset return and volatility spillovers, with application to global equity markets. *The Economic Journal*, 119(534):158–171.

Diebold, F. X. and Yilmaz, K. (2012). Better to give than to receive: Predictive directional measurement of volatility spillovers. *International Journal of forecasting*, 28(1):57–66.

Diebold, F. X. and Yilmaz, K. (2014). On the network topology of variance decompositions: Measuring the connectedness of financial firms. *Journal of Eeconometrics*, 182(1):119–134.

Diebold, F. X. and Yilmaz, K. (2023). On the past, present, and future of the Diebold-Yilmaz approach to dynamic network connectedness. *Journal of Econometrics*, *forthcoming*.

European Commission (2020a). Critical raw materials for strategic technologies and sectors in the EU - A foresight study. Available online at: `https://ec.europa.eu/docsroom/documents/42881`.

European Commission (2020b). Critical raw materials resilience: Charting a path towards greater security and sustainability. COM(2020) 474. Available online at: `https://ec.europa.eu/docsroom/documents/42849`.

Fally, T. and Sayre, J. (2018). Commodity trade matters. NBER Working Paper 24965, National Bureau of Economic Research.

French, K. R., Schwert, G. W., and Stambaugh, R. F. (1987). Expected stock returns and volatility. *Journal of financial Economics*, 19(1):3–29.

Graedel, T. E., Harper, E. M., Nassar, N. T., Nuss, P., and Reck, B. K. (2015a). Criticality of metals and metalloids. *Proceedings of the National Academy of Sciences*, 112(14):4257–4262.

Graedel, T. E., Harper, E. M., Nassar, N. T., and Reck, B. K. (2015b). On the materials basis of modern society. *Proceedings of the National Academy of Sciences*, 112(20):6295–6300.

Hoerl, A. and Kennard, R. (1988). Ridge regression. In *Encyclopedia of Statistical Sciences*, volume 8. Wiley.

Jacomy, M., Venturini, T., Heymann, S., and Bastian, M. (2014). Forceatlas2, a continuous graph layout algorithm for handy network visualization designed for the gephi software. *PloS one*, 9(6):e98679.

Koop, G., Pesaran, H. M., and Potter, S. M. (1996). Impulse response analysis in nonlinear multivariate models. *Journal of Econometrics*, 74(1):119–147.

Lèbre, É., Stringer, M., Svobodova, K., Owen, J. R., Kemp, D., Côte, C., Arratia-Solar, A., and Valenta, R. K. (2020). The social and environmental complexities of extracting energy transition metals. *Nature communications*, 11(1):4823.

Metcalf, G. E. (2014). The economics of energy security. *Annu. Rev. Resour. Econ.*, 6(1):155–174.

Nakano, J. (2021). The geopolitics of critical minerals supply chains. Center for Strategic and International Studies (CSIS). Available online at: `http://www.jstor.org/stable/resrep30033`.

Nicholson, W. B., Matteson, D. S., and Bien, J. (2017). VARX-L: Structured regularization for large vector autoregressions with exogenous variables. *International Journal of Forecasting*, 33(3):627–651.

Owen, J. R., Kemp, D., Lechner, A. M., Harris, J., Zhang, R., and Lèbre, É. (2022). Energy transition minerals and their intersection with land-connected peoples. *Nature Sustainability*, pages 1–9.

Pesaran, H. M. and Shin, Y. (1998). Generalized impulse response analysis in linear multivariate models. *Economics Letters*, 58(1):17–29.

Sovacool, B. K. and Brown, M. A. (2010). Competing dimensions of energy security: an international perspective. *Annual Review of Environment and Resources*, 35:77–108.

Tibshirani, R. (1996). Regression shrinkage and selection via the lasso. *Journal of the Royal Statistical Society: Series B (Methodological)*, 58(1):267–288.

U.S. Department of the Interior (2022). 2022 Final list of critical minerals. Federal Register, 87 FR 10381, 10381-10382. Available online at: `https://www.federalregister.gov/documents/2022/02/24/2022-04027/2022-final-list-of-critical-minerals`.

Yergin, D. (2006). Ensuring energy security. *Foreign affairs*, 85(2):69–82.

Zhang, L., Chen, Z., Yang, C., and Xu, Z. (2022). Global supply risk assessment of the metals used in clean energy technologies. *Journal of Cleaner Production*, 331:129602.

Zhu, X., Wang, W., Wang, H., and Härdle, W. K. (2019). Network quantile autoregression. *Journal of econometrics*, 212(1):345–358.

Zou, H. and Zhang, H. H. (2009). On the adaptive elastic-net with a diverging number of parameters. *Annals of Statistics*, 37(4):1733–1751.

A Descriptive statistics

Here we report the log of the realized volatility in standard deviations for the 16 ETMs over the entire sample (Figure A1) and additional information considering aggregation of the 16 commodities in three groups. In particular, Figure A2 shows the price indices and the RV for each group (base metals, precious metals, other ETMs).

Figure A1: Log realized volatility of energy transition metals: June 2012 - December 2022

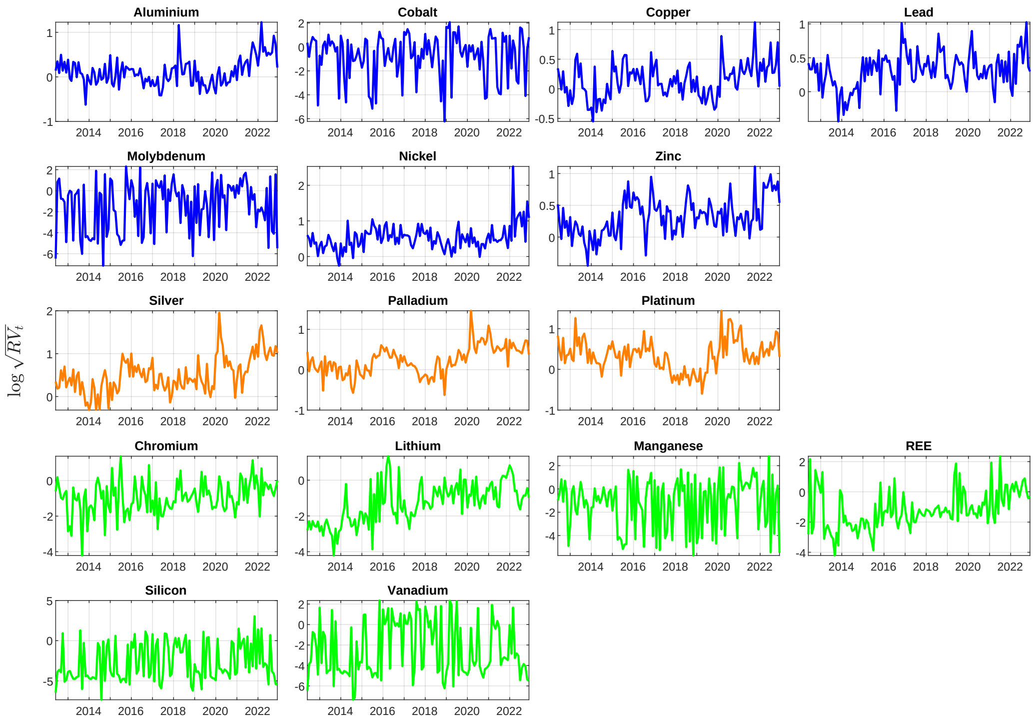

Figure A2: Energy Transition, Base, Precious and Other Metals: price indices and volatilities June 2012 - December 2022

(a) Price indices

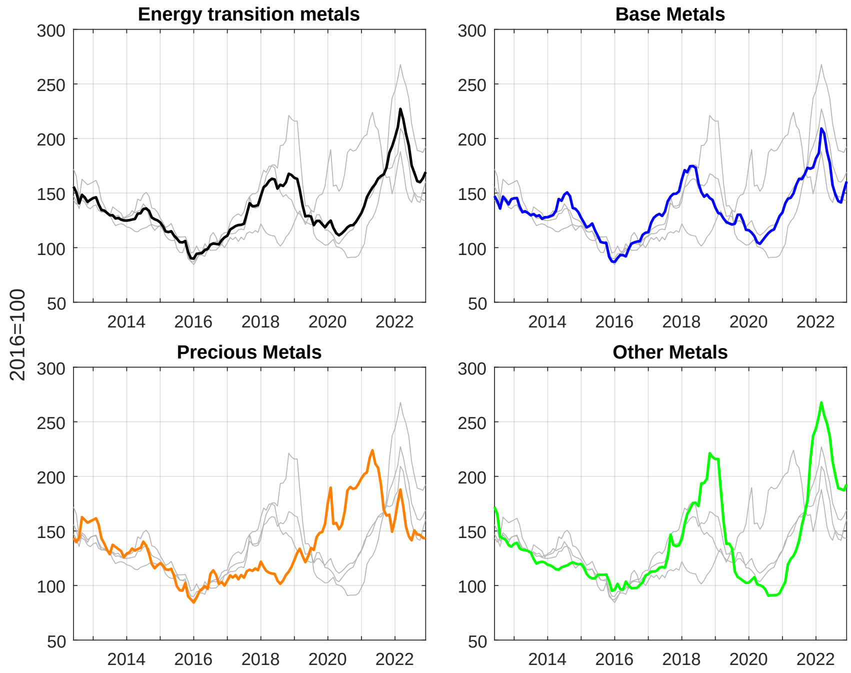

(b) Log Realized Volatilities

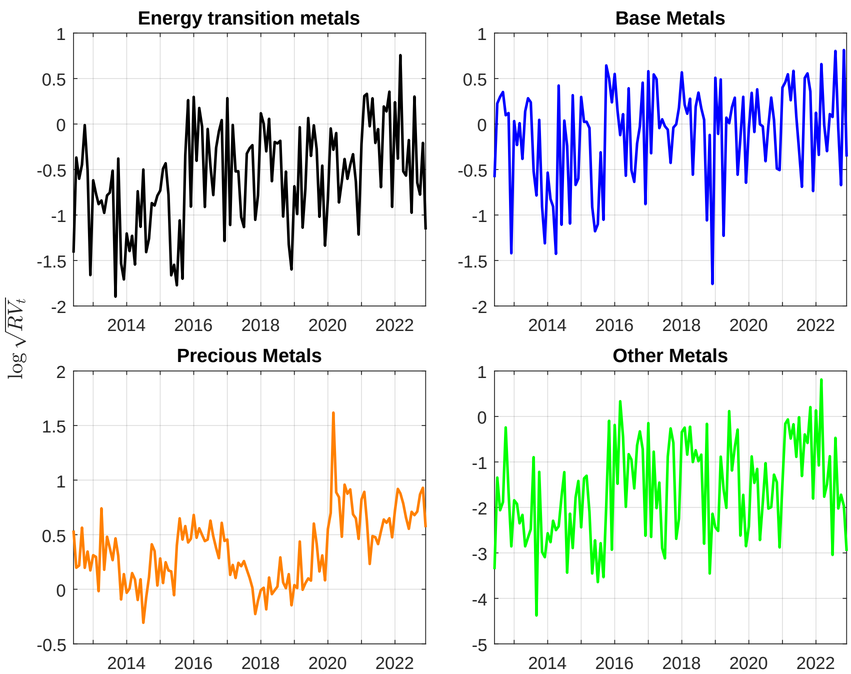

Notes: price indices and log realized standard deviations for each category of metals. Price indices and volatilities shown in the graphs are computed as cross-sectional averages of the underlying series. Prices have been normalized as follows: $100 \times P_{mt}/\bar{P}_m^{2016}$ where $\bar{P}_m^{2016}$ is the average price of m for 2016. Metal groups are defined in Table 1.

B Additional tables and figures

This Section reports the connectedness tables for eturns and RV of the 16 ETMs (Tables A1 and A2). Additionally, Figures A3 and A4 focus on from, to and net connectedness statistics for returns, not reported in the paper. Figure A5 disentangles the systemwide connectedness for returns and RV into within and between connectedness, obteined by considering group connectivity. Figure A6 shows the dynamics of the net connectedness by group over the rolling sample. Figure A7 reports the leads and lags correlation analysis between the estimated connectedness and some selected indicators of economic activity, uncertainty and supply-chain pressure. Finally, Figure 9 compares the Diebold and Yilmaz (2009, 2012, 2014) methodology with alternative measures of connectedness considering systemic risk (specifically Billio et al., 2012, considering Principal Components within a VAR).

Table A1: Connectedness table for returns

	Base							Precious			Other						
	Aluminium	Cobalt	Copper	Lead	Molybdenum	Nickel	Zinc	Silver	Palladium	Platinum	Chromium	Lithium	Manganese	REE	Silicon	Vanadium	From
Aluminium	36.57	0.13	12.38	10.66	0.79	6.80	12.47	2.25	4.19	3.65	1.84	0.99	0.91	2.43	3.55	0.40	3.96
Cobalt	1.57	72.17	1.42	1.82	2.88	1.03	1.10	0.66	1.16	0.92	0.27	0.31	11.32	1.36	0.36	1.65	1.74
Copper	10.83	0.03	31.43	11.27	0.02	7.15	15.78	4.82	9.18	6.11	0.67	0.05	0.64	1.55	0.17	0.31	4.29
Lead	10.08	0.42	12.33	34.55	0.17	8.08	14.53	4.23	5.53	7.82	0.33	0.12	0.01	1.31	0.07	0.43	4.09
Molybdenum	2.82	1.44	1.59	1.61	71.70	5.70	1.35	0.79	2.37	1.40	1.28	0.23	6.09	0.82	0.06	0.75	1.77
Nickel	7.45	0.06	8.87	9.40	2.39	38.20	6.69	5.72	8.26	9.96	0.02	1.19	0.07	0.89	0.46	0.37	3.86
Zinc	11.49	0.02	16.73	14.06	0.13	5.80	33.37	3.28	6.65	5.74	0.67	0.97	0.10	0.52	0.23	0.24	4.16
Silver	2.99	0.44	7.13	5.70	0.15	6.87	4.58	46.34	12.84	7.87	1.05	0.08	1.64	0.51	0.99	0.82	3.35
Palladium	4.13	0.01	10.37	5.71	0.56	7.53	7.07	9.83	35.35	18.16	0.00	0.17	0.01	0.61	0.15	0.34	4.04
Platinum	3.92	0.08	7.38	8.57	0.36	9.67	6.51	6.46	19.22	37.19	0.06	0.02	0.10	0.30	0.10	0.07	3.93
Chromium	4.52	1.01	1.95	0.78	1.85	0.26	1.75	1.77	0.17	0.13	77.60	0.85	3.32	0.53	0.47	3.04	1.40
Lithium	2.05	0.60	0.36	0.34	0.61	2.09	2.02	0.68	0.38	0.03	1.24	69.02	4.55	6.71	7.51	1.83	1.94
Manganese	2.98	5.31	2.88	1.54	5.93	1.08	1.34	2.51	0.87	0.90	2.23	0.27	68.66	2.02	0.36	1.10	1.96
REE	3.99	2.08	3.46	2.75	1.64	1.03	0.75	1.74	1.25	0.48	0.56	3.05	7.19	67.22	1.70	1.08	2.05
Silicon	5.96	0.50	0.56	0.21	0.34	0.35	0.62	1.09	0.29	0.13	1.07	0.09	2.45	1.97	84.07	0.31	1.00
Vanadium	1.05	4.80	0.74	0.95	3.44	0.83	0.54	1.52	0.78	0.22	0.63	1.73	3.10	1.73	0.27	77.67	1.40
To	4.74	1.06	5.51	4.71	1.33	4.02	4.82	2.96	4.57	3.97	0.74	0.63	2.59	1.45	1.03	0.80	**44.93**
Net	0.77	-0.68	1.22	0.62	-0.44	0.15	0.65	-0.39	0.53	0.04	-0.66	-1.30	0.63	-0.59	0.03	-0.60	-

Notes: full sample connectedness. Entry in bold is total connectedness.

Table A2: Connectedness table for volatilities

	Base							Precious			Other						
	Aluminium	Cobalt	Copper	Lead	Molybdenum	Nickel	Zinc	Silver	Palladium	Platinum	Chromium	Lithium	Manganese	REE	Silicon	Vanadium	From
Aluminium	47.15	0.02	11.18	4.23	0.23	10.11	8.35	9.64	2.88	1.05	0.71	0.27	0.59	2.43	1.10	0.08	3.30
Cobalt	0.05	75.93	0.86	0.12	6.92	3.11	0.37	0.32	1.63	0.12	0.75	0.03	4.16	0.59	2.24	2.80	1.50
Copper	8.26	0.39	34.86	8.75	0.71	8.03	10.51	11.73	9.01	3.81	2.71	0.71	0.17	0.24	0.05	0.08	4.07
Lead	3.99	0.07	11.18	44.54	0.20	6.14	21.17	5.36	4.05	0.81	0.78	0.58	0.38	0.70	0.00	0.04	3.47
Molybdenum	0.37	6.72	1.45	0.31	70.30	0.31	0.69	0.17	1.26	0.02	0.19	0.31	12.16	0.12	1.40	4.22	1.86
Nickel	9.37	1.77	10.06	6.02	0.17	43.69	10.48	7.05	4.38	0.37	3.76	0.32	0.02	0.64	1.23	0.67	3.52
Zinc	6.30	0.17	10.74	16.92	0.34	8.54	35.61	9.79	5.67	1.23	1.11	1.49	0.08	1.90	0.01	0.08	4.02
Silver	7.15	0.14	11.76	4.21	0.07	5.64	9.61	34.95	14.58	4.93	1.10	2.25	1.05	2.55	0.02	0.01	4.07
Palladium	2.30	0.81	9.72	3.42	0.65	3.77	6.00	15.69	37.62	13.52	0.55	2.50	0.23	3.15	0.05	0.02	3.90
Platinum	1.29	0.09	6.36	1.06	0.03	0.50	2.00	8.19	20.88	58.10	0.06	0.43	0.31	0.33	0.12	0.25	2.62
Chromium	1.14	0.79	5.69	1.29	0.42	6.33	2.30	2.32	1.10	0.08	73.15	1.03	1.41	0.32	2.21	0.43	1.68
Lithium	0.64	0.09	1.50	1.02	0.30	0.69	3.23	4.73	5.08	0.54	0.92	73.86	1.52	2.98	2.65	0.26	1.63
Manganese	0.89	3.52	0.33	0.56	11.86	0.08	0.16	1.99	0.43	0.35	0.71	1.11	66.87	0.50	6.85	3.80	2.07
REE	3.73	0.64	0.54	1.15	0.41	1.09	3.89	5.29	6.09	0.39	0.32	2.19	0.76	70.89	2.49	0.12	1.82
Silicon	1.58	2.38	0.16	0.01	3.20	1.88	0.04	0.14	0.19	0.09	0.88	0.97	6.68	2.13	65.82	13.86	2.14
Vanadium	0.12	3.84	0.22	0.08	6.08	1.17	0.21	0.03	0.12	0.09	0.18	0.26	2.50	0.04	14.91	70.16	1.87
To	2.95	1.34	5.11	3.07	1.97	3.59	4.94	5.15	4.83	1.71	0.92	0.90	2.00	1.16	2.21	1.67	**43.53**
Net	-0.35	-0.16	1.04	-0.39	0.12	0.07	0.91	1.09	0.94	-0.91	-0.76	-0.73	-0.07	-0.66	0.07	-0.19	-

Notes: full sample connectedness. Entry in bold is total connectedness.

Figure A3: Full sample group connectedness measures for returns

(a) Within and cross group connectedness (b) To, from and net connectedness

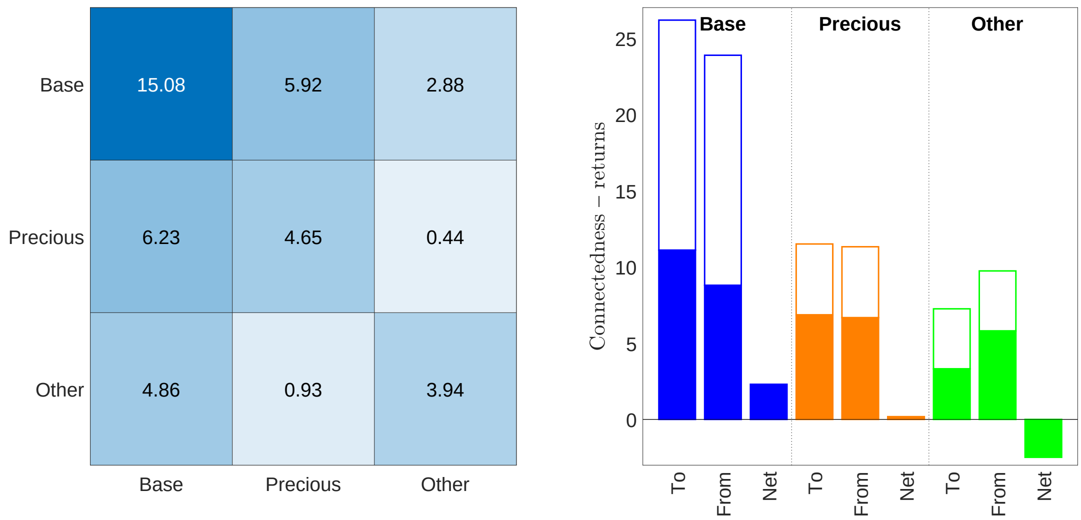

Notes: panel (a) shows within group connectedness along the main diagonal, while off-diagonal elements are cross group connectedness measures. Panel (b) shows the to, from and net connectedness statistics for groups of metals. Colored areas refer to the off-diagonal statistics, whereas the white areas denote statistics comprehending the diagonal elements

Figure A4: To, from and net connectedntess – returns

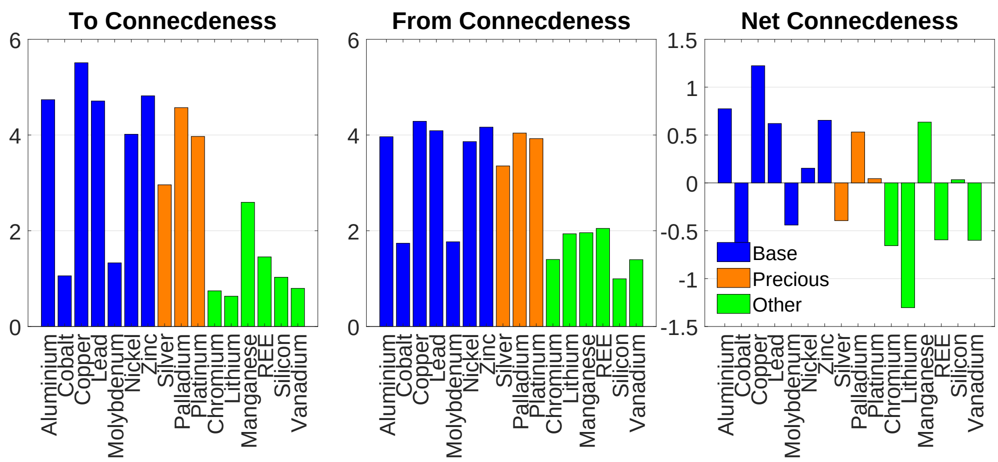

Figure A5: Time-varying Connectedness: total, within and between groups

(a) Returns

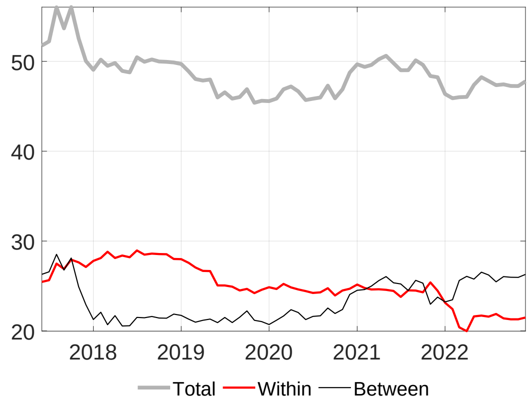

(b) $log\sqrt{RV_t}$

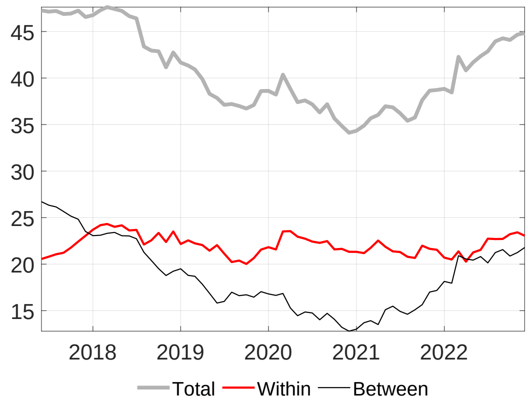

Figure A6: Time-varying net connectedness by groups

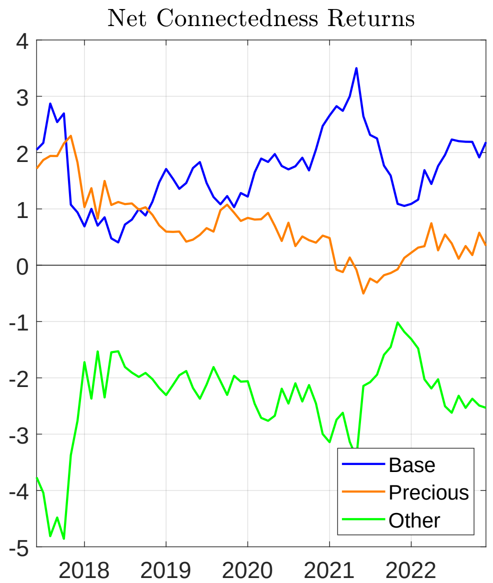

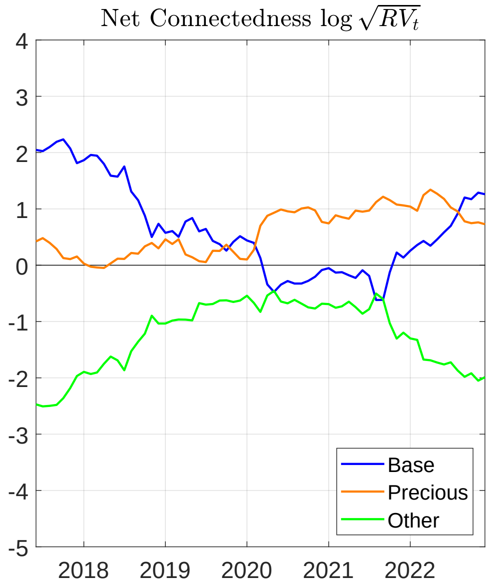

Figure A7: Leads and Lags correlation analysis

(a) Returns connectedness correlation (b) $log\sqrt{RV_t}$ connectedness correlation

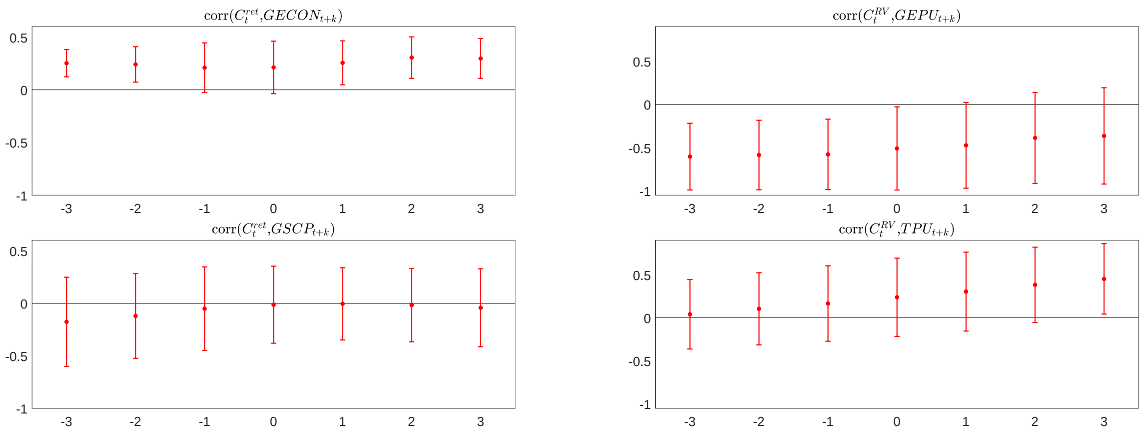

Notes: red bars highlights the correlation coefficient and relative standard deviations for different leads (k up to 3) and lags (k up to -3).